Available online at www.sciencedirect.com
SCIENCE DIRECT
Fire Safety Journal 41 (2006) 171–184
FIRE SAFETY JOURNAL
www.elsevier.com/locate/firesaf

Instrumentation of wildland fire: Characterisation of a fire spreading through a Mediterranean shrub

P.A. Santoni*, A. Simeoni, J.L. Rossi, F. Bosseur, F. Morandini, X. Silvani, J.H. Balbi, D. Cancellieri, L. Rossi

SPE – UMR CNRS 6134, Université de Corse, Campus Grossetti, B.P. 52, 20250 Corte, France

Received 23 February 2005; received in revised form 15 September 2005; accepted 30 November 2005
Available online 3 February 2006

Abstract

Although considerable progress has been made recently in the modelling of the spreading of a forest fire, there remains a lack of reliable field measurements of thermodynamic quantities. We propose in this paper a method and a set of measuring structures built in order to improve the knowledge of the fundamental physical mechanisms that control the propagation of wildland fires. These experimental devices are designed to determine: the fire front shape, its rate of spread, the amount of energy impinging ahead of it, the vertical distribution of the temperature within the fire plume as well as the wind velocity and direction. The methodology proposed was applied to a fire spreading across the Corsican scrub on a test site. The recorded data allowed us to reconstruct the fire behaviour and provide its main properties. Wind and vegetation effects on fire behaviour were particularly addressed.

Keywords: Instrumentation of wildland fire; Field experiments; Fire behaviour; Fuel characteristics

1. Introduction

Fire spread models have been classified [1] as statistical, empirical and physical models, according to whether they involve no physics at all; no distinctions between the different modes of heat transfer (conduction, convection and radiation), or account for each mechanism of heat transfer and production individually. The purpose of statistical and empirical models is mainly restricted to the prediction of the rate of spread. They do not use any physical modelling to describe the heat transfer from the burning zone to the unburnt fuel. These models may be very efficient for fuel and environmental conditions comparable to those of the test-fires used to tune them but the absence of a real physical description make them inapplicable in other situations. On the basis of a detailed description of the heat transfer mechanisms, which govern the fire propagation, the physical models possess a great generality, which makes them efficient in most fire situations. Among them, the two-phase models consider a gas phase flowing through a bed, which is viewed as an agglomeration of organic, randomly oriented fuel elements. Since the pioneering work of Grishin [2] these models are becoming more and more detailed as illustrated by [3–6]. The only measurements available to test these models were coarse observations of the visible flame length or rate of spread at the laboratory scale [7]. Then, the lack of measurements of flame properties in wildland fuels was partly addressed in a paper of Marcelli et al. [8] devoted to the test of the two-phase approach developed by Porterie et al. [7]. In this last laboratory work, gas temperature and velocity distributions within a flame spreading across a fuel bed were measured and compared to the simulation results of the two-phase model.

However, as our knowledge stands at present, comparisons between the predictions of two-phase models and field experimental results do not exist. Two reasons can be found to explain this lack of comparisons. The first one lies in the complexity of the two-phase models. At small or medium scale (length scale of about 100 m) this approach is limited until now to line fires, for which a two-dimensional

*Corresponding author. Fax: +33 495 450 162.
E-mail address: santoni@univ-corse.fr (P.A. Santoni).

0379-7112/$ - see front matter © 2006 Elsevier Ltd. All rights reserved.
doi:10.1016/j.firesaf.2005.11.010

(2D) approximation in a plane defined by the direction of propagation and the vertical is made [9]. Hence, the most relevant data available in the literature for field experiments, such as the fire front shape, curvature and width cannot be used to validate the simulation of such 2D models. Cheney et al. [10,11] have, however, identified fire front shape as a significant variable influencing fire spread, which must be taken into consideration, when using experimental fires to validate models. Then, caution should be exercised when those models predict rate of spread since it highly depends on shape and size of the fire front under wind and slope conditions. At this stage, it should also be mentioned that numerical calculations performed for a real fire configuration have shown the interest of coupling an atmospheric boundary layer model with a propagating heat source representing a wildfire front [12]. In spite of the simplified character of the formulation (the combustion is not directly calculated), the fact of taking into account the modifications generated by the buoyancy driven flow on the local wind allows the quality of the predictions delivered by the model (rate of spread, wind and slope effects…) to be improved considerably. One can thus speculate on the relevance of the simulation results carried out in a 2D formulation neglecting the atmospheric influence. This important feature was also pointed out by [13], who developed FIRETEC, a coupled atmospheric transport/wildfire behaviour model, at Los Alamos National Laboratory. The second reason for few comparisons between two-phase models and data from field experiments lies in the lack of reliable field measurements of thermodynamic quantities, which are the pertinent outputs of the two-phase formulations. The need for accurate and relevant experimental data on fire spread and related phenomena, in order to check modelling hypothesis or to validate existing models is commonly felt among the scientific community. A lot of experimental fires have been conducted at the field scale by scientific and research teams [10,11,14–17]. However, thermodynamics quantities allowing characterising fires in field experiments from a physical viewpoint were scarcely investigated by researchers [17,18]. Furthermore, a common protocol has not yet been defined by the scientific community to describe and characterise such fires apart from common behaviour descriptors such as: the visible flame properties (flame height, flame tilt angle, flame depth etc…), the flame residence time, the Byram's fireline intensity [19] and the fire front shape.

Forest fire is a complex phenomenon in which the levels of description cover a huge range, from the details of the kinetics of gaseous combustion and thermal degradation of fuels, up to the physical–chemistry characterisation of flames and vegetation cover as a fuel. The aim of this work is to propose a method and a set of measuring structures built in order to improve the knowledge of the fundamental physical mechanisms that control the propagation of wildland fire. The topics covered here are concerned with the behaviour descriptors previously mentioned and the measurements of the thermodynamic quantities involved in forest fires. Among them, they include the determination of the fire front shape and its rate of spread, the measurement of the amount of energy impinging ahead of it, the characterisation of the vertical distribution of the temperature within the fire plume, as well as the measurement of the wind velocity and direction. Other parameters are also relevant to fire behaviour analysis but they are not addressed in the current paper. Among others, there are spotting, air quality measurements, fire retardant efficiency assessment studies [20] and so on. The methodology proposed was applied to a fire spreading across the Corsican scrub on a test site. The recorded data allowed us to reconstruct the fire behaviour and to provide its main properties. Wind and vegetation effects on fire behaviour, which are mainly responsible of the hazards encountered in forest fires, are particularly addressed in this paper. These results are presented, as well as the characterisation of the vegetative structure, which can be used to validate and tune models of fire spread at the field scale.

2. Site description

2.1. Site location and preparation

The experiments were carried out in South Corsica coastal region near Porto-Vecchio. In the past, this area was frequently submitted to several catastrophic wildfires, which lasted several days and burned thousands hectares of scrub. Most of them occurred in summer under western windy condition (greater than 12 m/s), high ambient temperature (greater than 30°), low relative humidity (lower than 30%), low fuel moisture content and drought conditions. The test site was selected in this area in order to get simultaneously some of those conditions for which high intensity fires occurred. Although many of the environmental factors affecting severe fire occurrence have already been recognised [21], it has been observed that there is not some constant prevailing. Instead there is a mixture of several danger variables, which together combine to produce conditions for a major fire to occur [22]. Our aim was to reproduce these conditions through a small-scale field experiment involving a spreading fire, representative of weather and fuel state conditions encountered in severe fires. However, it is recognised that it is impossible to duplicate an actual wildfire. Those conditions were firstly necessary to test our method and our set of measuring structures and secondly to bring more insight on the knowledge of the fundamental physical mechanisms that control the propagation of wildland fire.

The experimental burning plots were established in private lands, the owners of which gave us permission to burn. This site (see Fig. 1) was chosen by our public partners of the French Forest Service and the Fire Brigade Service since it is delimited by a huge fuel break (fuel break is a fire containment method) on one side, which facilitates the safety conditions. The layout of the plots was designed by taking into account the experimental requirements, the

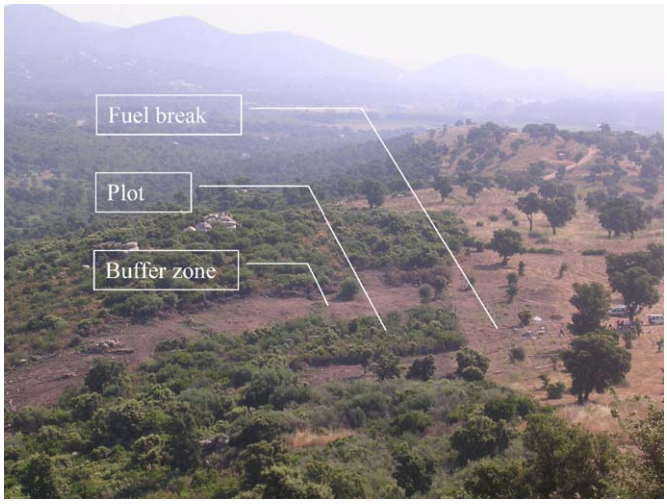

Fig. 1. General view of the selected plot.

terrain configuration and the safety conditions. Concerning the experimental requirements, a first plot was especially designed to test the different measuring structures developed by our team. It was a small square of 15 m sides located on even terrain. A second plot was devoted to study the fire behaviour. Situated on uneven terrain, it was in the shape of a rectangle, 30 m wide perpendicular to the slope with a northwestern outlook on that side and 80 m long parallel to the slope (cf. Fig. 1). The 30 m wide upper limit of that rectangle was delimited by the fuel break. Along the longest sides, the first 50 m were under upslope condition while the 30 remaining meters were on flat terrain. For each plot, a safety belt of 20–30 m wide was build with a bulldozer. This buffer zone between the plots and the surrounding vegetation was necessary first of all to preserve the integrity of the personnel but also to prevent any fire breakout, which could be disastrous in summer. The results presented hereafter will concern the burning of the second plot.

2.2. Topography

As part of this experience, it was very important to have an accurate altimetry model at one's disposal. Due to the small dimensions of the experimental site, we could not use an existing Digital Elevation Models (DEM) such as, for example, BDAlti® of the Institut Géographique National (IGN), which have a spatial discretisation of 25 m. We thus carried out a precise topographic statement of the parcel which was necessary, on the one hand, for the construction of a DEM and, on the other hand, to integrate data into a Geographic Information System (GIS). In order to obtain the best accuracy, we used a Leica tachometer for the topographic statements. Because of the density of the vegetation, we waited until after burning to do measurements. We built the DEM from the points raised by the tachometer, thanks to a spline interpolator—a general-purpose interpolation method that fits a minimum curvature surface through the input points. This method is best for gently varying surface such as elevation. The DEM obtained was very close to the reality.

In order to study the spatial distribution of the vegetation on the parcel, we integrated the data coming from site survey within a GIS. The layers obtained from the census, described hereafter, were scanned and georeferenced. Then, we used a semi-automatic vectorisation method to obtain polygonal vector layers for the different strata of vegetation. In addition to spatial data, attribute data were also stored in the tables that contain the descriptive fields (species, minimum/maximum dimensions, recovery rate…).

2.3. Vegetation cover

Before the burning, we took an inventory of the vegetation located on the parcel with the aim of obtaining a qualitative and quantitative description of species before the experiment. We built a statistical description by species and by class of vegetation and we generated a GIS cartography. To map vegetation, we used a quadrat method by dividing the parcel in 90 quadrats of 25 m^2. In each quadrat, we measured the location of each species and their heights. Vegetation was classified in a flora. The shrub layer represented the most part of the vegetation cover. Dominant species were olive tree (*Olea Europaea*), strawberry tree (*Arbutus Unedo*) and white heath (*Erica Arborea*). There were also notable amounts of cistus (*Cistus Monspeliens*), golden-chain (*Cytisus Triflorus*) and oak (*Quercus Ilex*). The mean height of vegetation ranged between 2 and 3 m. The herbaceous layer was sparsely distributed on the parcel mainly due to the presence of a dense shrub layer. Vegetation was also classified in strata: upper shrub layer (>2 m), lower shrub layer (<2 m) and herbaceous layer (see Table 1). The community studied showed a total cover of practically 100%. The upper shrub layer represented 15% of the cover of the parcel, the lower one 85% and the herbaceous layer 5% (located under the two shrub layers). We measured moisture content for each species just before conducting the experimental fire. To proceed, we collected samples of leaves in the vegetation neighbouring the parcel. These samples were oven-dried at 60 °C for 24 h and the fuel moisture was expressed as a percentage of dried weight. We can note high values for

Table 1
Vegetation heights and moisture contents for some species

Species	Minimal height (m)	Maximal height (m)	Moisture content (%)
Olea Europaea	2.13	3.26	84
Quercus Ilex	1.45	2.89	67
Arbutus Unedo	1.11	2.29	108
Cistus monspeliens	0.93	2.01	78
Cytisus triflorus	0.58	1.50	100

moisture contents (see Table 1). This was mainly due to the rainy conditions in spring before the experiment.

The entire variables described here before were integrated in a GIS in order to obtain a detailed description of the vegetation of the parcel.

2.4. Pre-burn meteorological conditions

Among the conditions under which large fires are more likely to occur, an important role is played by weather factors and meteorological phenomena: strong surface wind, drought condition and so on [22]. Weather variables are thus of extreme importance and should be surveyed in order to plan both the day and the time of the experimental burns. A weather Campbell® automatic station was installed in the study area 2 months before the experiments in order to gather data on the local meteorological conditions. It was located slightly below the second plot and recorded the following parameters every minute: average air temperature, average relative humidity, average wind speed at 2 m high above ground level and average wind direction.

The recorded data revealed two regimes for the wind speed and direction over the plot. The first one, which is the most frequent is an easterly regime due to a sea breeze effect. It is quite strong during daytime in the eastern faç ade of Corsica. The second one is a westerly regime due to large-scale atmospheric circulation. It takes place mainly during the night and after 16:00 when the sea breeze effects cease. These two regimes clearly appear on Fig. 2, which represents the compass card of the plot between 12:00 and 18:00 for 16 days before the burning day (July 2). They

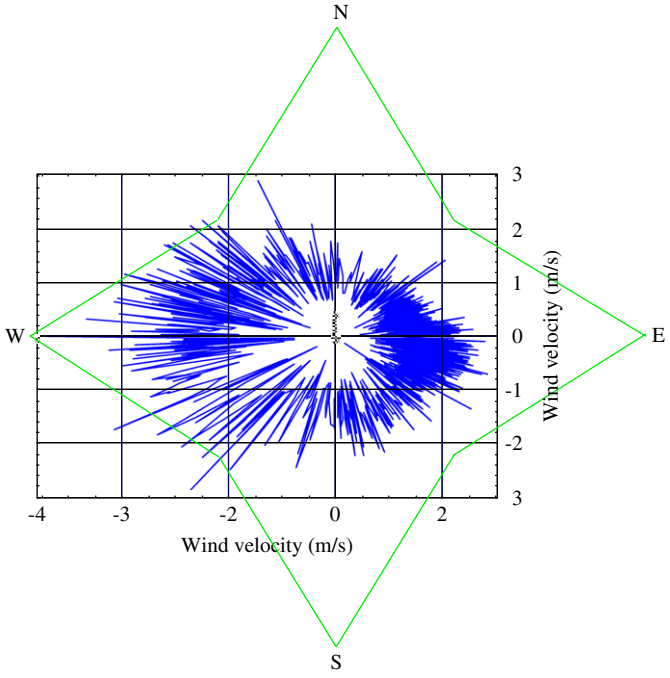

Fig. 2. Compass card of the plot between 12:00 and 18:00 for 16 days before the burning day (July 2).

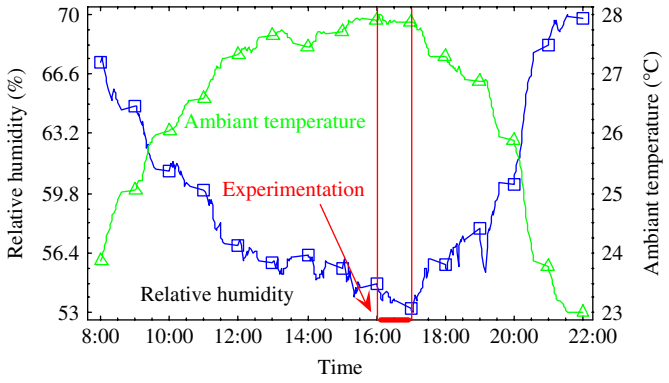

Fig. 3. Average daily dynamics of air temperature and relative humidity for 16 days before the burning day (July 2).

possess distinct scales in space and time and lead more often to the establishment of a surrounding circulation dominated by east wind with high humid contents. Under these humid conditions the occurrence of severe fires in east Corsica is inhibited. Conversely, the disruption of east wind regime creates west wind and results in dryer air, which favors the occurrence of wildfires. We can note that the wind velocity is higher for the westerly regime than for the easterly one, increasing the fire danger. Fig. 3 displays the averaged daily dynamics of air temperature and relative humidity recorded on the plot for 16 days before the burn. All these data were combined in order to select the best period of the day to burn between 16:00 and 18:00, since we expected to have simultaneously high west wind with high air temperature and low relative humidity values.

3. Experimental method and apparatus

3.1. General overview of the experimental protocol

As mentioned above, the plot was in the shape of a rectangle, 30 m wide perpendicular to the slope with a northwestern outlook on that side and 80 m long parallel to the slope. Its orientation, according to slope and west winds, was managed to result in better chances of achieving a fire spreading as similar as possible to the previous high intensity fires that occurred in that place. The burning strategies were as follows (Fig. 4): without wind, a linear ignition would be performed at the bottom of the plot (resulting in a fire driven by the slope) and under west windy condition, a point ignition would be performed on the right side of the plot (resulting in a fire driven by the wind under no slope). The experimental protocol was elaborated in order to investigate two sets of fire behaviour variables. The first one concerns the properties of the fire front itself and its changes during the spreading according to the environmental conditions. The second one is related to the effects of the fire front on the area ahead of it. To this end, different measuring structures and devices were developed. They are depicted hereafter and displayed in

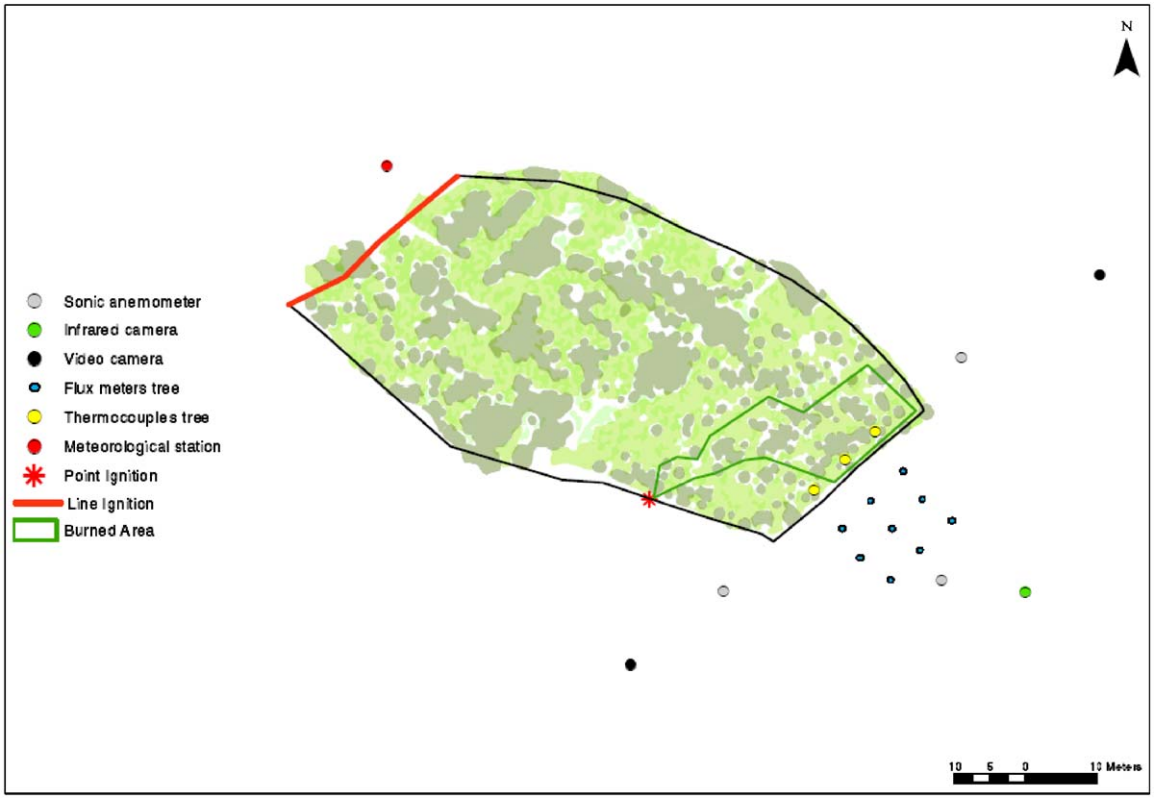

Fig. 4. Map of protocol application.

Figs. 4 and 5, which present the overall experimental set-up.

With regard to the investigation of the properties of the fire front, several devices were located inside the vegetation and along the longest sides of the plot. The first series of devices, named in the following as "characterisation lines", were developed to determine the fire front perimeter over time. The second ones, called "thermocouple trees", are measuring structures of 6 m high built in order to study the temperature in the fire plume (Fig. 5). Some thermocouples were also put on the ground to assess the fire residence time. Three 2D sonic anemometers were placed around the parcel in order to record the surface wind entering the plot (Fig. 5). The first two were located on the right and left sides of the parcel at 2 m height while the third one was positioned in the fuel break ahead of the upper limit of the plot. Two video cameras were located on the sides (Fig. 4) to survey the fire and investigate the flame shape (height, length, depth and tilt angle). Those last data were also evaluated by two pairs of experienced observers walking parallel to the fire front main direction of propagation.

Concerning the study of the fire front effects on the area ahead of it, nine posts, each one containing four heat flux sensors, were placed in the fuel break ahead of the upper limit of the plot in order to record the radiant and total heat flux (Fig. 5). An infrared camera and a video camera were used to film the fire font reaching the thermocouple trees in a frontal view and a remote video camera served to localise the fire front advance. Finally, a weather station

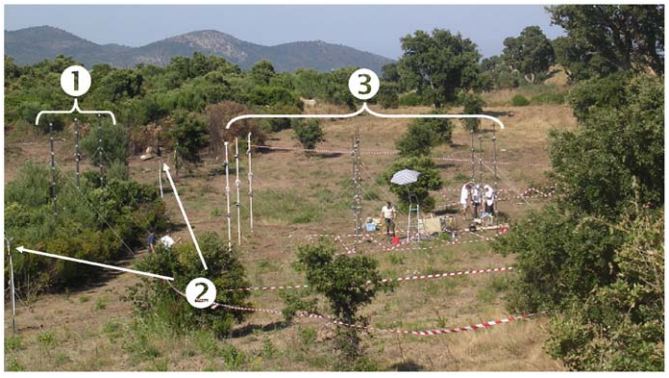

Fig. 5. Measuring structures for thermodynamic quantities (① Thermocouple trees, ② Sonic anemometers, ③ Flux meters trees).

was located at the bottom of the parcel to record the weather variables as previously mentioned (Fig. 4).

3.2. Determination of the fire front perimeter over time

At the field scale, the determination of the fire front perimeter as a function of time is tricky because of the visibility problems induced by factors such as smoke and vegetation structure. To circumvent those difficulties, we have developed a device, called a "characterisation line", devoted to detect the fire front advance. Such a device is displayed in Fig. 6. It consists of six sensors provided by a 12 V direct power supply. A sensor, numbered i, is

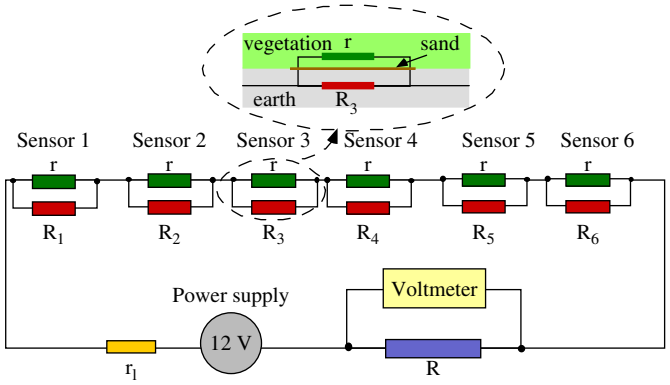

Fig. 6. Scheme of a "characterisation line" used to determine the fire front shape.

composed of two elements: a fuse, which breaks at 300 °C and whose resistance value is r, and a resistor, whose resistance value is R_i (with $r \ll R_i$). The fuses are located in the vegetation 15 cm above the ground and the resistors are buried in the ground, 20 cm deep. A voltage measurement is taken at the terminals of a charge resistor R. This voltage is $12.R/r_1 + R + 6r$ volts (where r_1 represents the value of the resistance of the wires) when all fuses short-circuit the resistors. When the fire front reaches a fuse, it will break while the corresponding resistor remains intact. In the case of sensor 1, for example, the value of the voltage is $12.R/r_1 + R + R_1 + 5r$ volts, once fuse 1 has melt. This voltage measurement makes it possible to accurately determine the instant of arrival of the fire front at the location of each sensor, provided that the resistances R_i possess different values. Six characterisation lines were placed in the upper part of the plot in order to mesh it as homogeneously as possible in spite of the difficulties encountered when entering into the shrub layer. Cross-checking between the measurements delivered by those devices and video recording would allow reconstructing the fire front perimeters over time.

3.3. Measurement of the vertical distribution of the temperature within the fire plume

Up to now, studies on the vertical distribution of the temperature within static [23] and spreading fire plumes [8,24] were mainly conducted at laboratory scale. Although these previous works brought some insight on flaming combustion of vegetative fuels, conversely they involved low fuel load for spreading fires (lower than 1.0 kg/m^2 in general) and small quantities of fuel (lower than 500 g in general) for static fires. Therefore, their results could not be extrapolated to actual wildland fuel structures such as Mediterranean shrub. Similar experiments in this vegetation type are almost inexistent at the field scale apart from [25], which investigated fire as a heat source to the atmosphere. These authors measured the vertical distribution of temperature originating from a combustion pile 16 m in diameter and 2.5 m high.

In the present work, three measuring structures of 6 m height were built in order to evaluate the temperature profile within the fire plume during the propagation. These masts were placed in the upper part of the plot, inside the vegetation (① in Fig. 5), and set at a distance of about 6 m from each other. Those locations were selected to provide a relevant characterisation of the flames when the fire front reaches the limit of the area devoted to investigate the radiant and convective heat transfers ahead of it. The main purpose of the "thermocouple trees" was to investigate whether the classical structure of the fire plume revealed by laboratory experiments [8] remains valid at field scale.

The flames encountered in free burning forest fires are typical diffusion flames in which one can distinguish three behavioural regions. The lower part of the fire plume is the continuous flame region close to the source of the fire. Above that region, there is the intermittent one where balls of flame come away from the source, and the upper part is the conventional thermal plume. In this present study, the measuring devices only investigated the lower and intermittent regions.

Each "thermocouple tree" was equipped with 10 thermocouples set at a distance of 0.6 m from each other (see Fig. 7) and positioned at the following heights: 0.6; 1.2; 1.8; 2.4; 3.0; 3.6; 4.2; 4.8; 5.4 and 6 m. The thermocouples used in these experiments were mineral-insulated integrally metal-sheathed (MIMS) pre-welded type K (chromel–alumel) pairs of wire with an ungrounded junction. The MIMS form of thermocouple consisted of matched thermocouple wires surrounded by insulating material compacted by rolling until the sheath is reduced in diameter. In this work, we used cheap stainless steel sheathed (304 SS) and MgO insulated standard thermocouples (Omega Engineering). The thermocouples were 15 cm long with sheaths of 250 μm in diameter and wires of 50 μm in diameter inside. These sensors were chosen since they constituted a compromise between their robustness and their rapidity (time constant of about 0.1 s). Then, each thermocouple was threaded through an insulator (13 cm long), made of recrystallised pure alumina ceramic containing over 99.8% Al_2O_3. The insulators protected the thermocouples' stainless steel sheaths. The flame could warm their sheaths without this protection and might well alter the measurements. Furthermore, both insulators and thermocouples were placed in stainless steel tube (see Fig. 7) devoted to protect the whole probes from twigs and physical contacts. The thermocouples protrude 20 mm from this set-up. The different parts of the measuring structures were thus designed and protected in view of the expected high temperatures. The cables were placed inside the "thermocouple tree" and were protected from the fire effects by putting them in an envelope made of two ceramic fibre sheets. The effects on the hydrodynamics and hence on the recorded temperature were assumed negligible.

The thermocouples were connected to a Hewlett Packard (HP E9811B) data logger, which is a programmable unit. It possesses an on-board digital signal processor, which converts the voltage read across the analog input channel

Fig. 7. Measuring structure for gas temperature: mast and set-up for the thermocouple protection.

and applies a high-speed conversion, providing measurements of temperature. The sampling frequency was 100 Hz and the precision in temperature measurement was 0.5 °C.

3.4. Weather parameters measurements during the burn

Weather parameters were recorded during the fire by the meteorological station previously mentioned but particular attention was given to gather supplementary data on wind field in the vicinity of the plot thanks to the three 2D sonic-anemometers (② in Fig. 5). The advantage of those anemometers lies in their sampling frequency of 1 Hz, which allows coping with possible quick changes of wind field that might affect fire behaviour. The anemometers were close enough to the plot to properly capture the relevant wind field acting on the fire while being aware that the fire itself could influence those measurements.

3.5. Measurement of the amount of energy impinging ahead of the fire front

Nine posts, each one supporting two devices containing two radiant and convective heat flux sensors (Captec®), were placed in the fuel break (③ in Fig. 5). On each post, the devices were located at two measurement heights—2 and 4 m—to represent, respectively, the height of a standing person and the height of the lower edge of a roof. The posts were positioned in three lines located at a distance of 5, 10 and 15 m from the top of the parcel, in order to investigate the heat flux variation along distance. Three following posts were lined up with each "thermocouple tree" in order to correlate the received heat fluxes with the fire plume.

3.6. Infrared camera

In order to characterise further the fire front reaching the top of the parcel, we used an infrared camera (CEDIP—Jade3MW), operating in the MIR band (from 3 to 5 μm) and located at 30 m from the upper limit of the plot (cf. Fig. 4). The camera has a 256×256 focal plane array and infrared images were stored on a PC. The acquisition rate was 25 images per second. We used a filter for CO_2 species (specified wavelength near 4.3 μm), to focus the measurements on the gas phase. The infrared camera allowed us to obtain measurements of the characteristic length scales of the fire front and pictures of flames with low smoke distortion. The results provided by the camera will be discussed in a subsequent paper.

4. Results and discussion

We encountered some difficulties in planning the burn since there was a rainy spring in 2004. Due to those exceptional rainfalls, live fuel moisture content was greater than usual in spring and we did not have acceptable conditions to manage the first scenario planned in the protocol (a linear ignition performed at the bottom of the plot resulting in a fire driven by the slope). Hence, we planned to carry out the burn of the plot in early summer under a western wind. This was necessary firstly to ensure lower moisture content in the live fuels and secondly to achieve our experimental requirement. That is to say, to obtain a fire under conditions for which catastrophic huge fires occurred during the past. We got an exceptional permission to burn the plot during the wildfire season and the fire was conducted on July 2. It was performed between 16:33 and 16:59, within the period of the day during which highest wind speeds (up to 8 m/s), high air temperature (32 °C) and minimum relative humidity (38%) values were recorded.

4.1. Time history of the fire front

A point ignition was performed on the right side of the parcel along the windward edge of the plot in order to exploit the overall measuring section under westerly wind conditions (see Fig. 4). The ignition process started at 16:33 and the fire burned for approximately 26 min. The time history of the fire propagation, based upon the remote

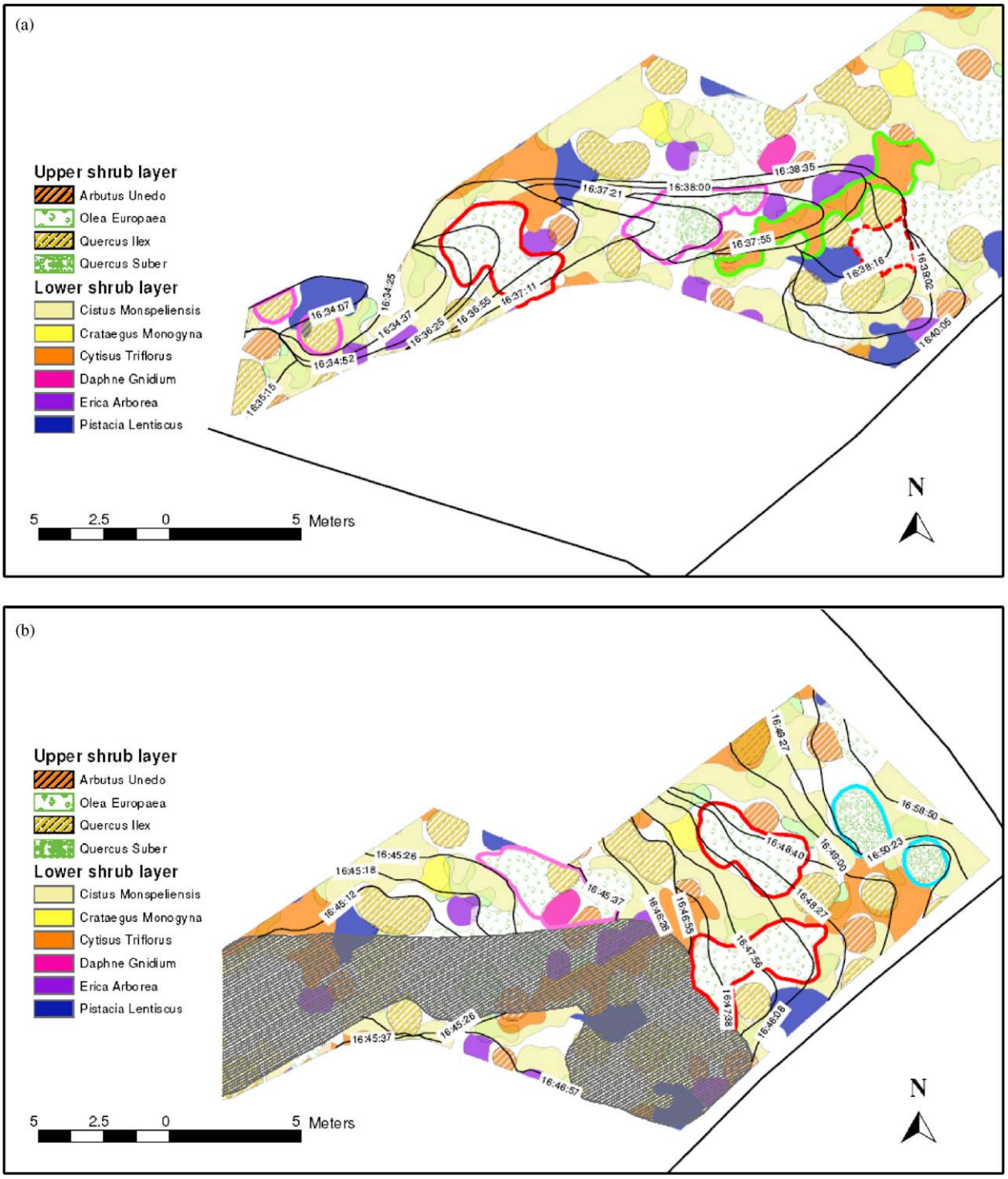

Fig. 8. Vegetation cover and diagram of the fire perimeters over time for the first head shape (a) and the second head shape (b).

imagery and ''characterisation lines'', data analysis is provided in Figs. 8a and 8b. It should be mentioned that the visibility problems induced by factors such as smoke and vegetation structure did not allow delivering a fire perimeter map from the video analysis only. A cross check between the ''characterisation lines'' measurements and video recording was necessary to reconstruct the fire front perimeters over time.

Figs. 8a and 8b show that the fire developed into two distinct head shapes over time. The overall burned area corresponding to Figs. 8a and 8b is displayed on Fig. 4. At the beginning, the fire burned with little variation in direction and few changes in speed. It took a narrow shape at the head (see Fig. 8a at time 16:37:11). A first change in wind direction causes part of the right flank to become a heading fire with a parabolic shape (Fig. 8a at time

16:38:00). The fire reached the limit of the plot and stopped due to the absence of fuel. Then after a lull in wind which last about 4 min, the wind speed increased and changed again in direction. This causes part of the left flank to become a heading fire with a broad parabolic shape (see Fig. 8b). It spread like a solid wall of flames, creating very high flames and potential danger of spotting (Fig. 8b at time 16:48:27). Short-distance (15–30 m) spotting occurred in the fuel break at that time. The fire propagation rate was variable, but generally ranged from 0.1 to 0.4 m/s. That sort of fire growth with changing head fire shape has already been pointed out by [11]. Their experiments, which were conducted in grasslands, showed that a fire may develop in a step-wise pattern with increases rate of spread being associated with shifts in wind direction and with a wider effective head fire. Although our experiment reveals the same behaviour concerning the wind shift influence on the fire front shape, conversely the increase in rate of spread with a wider effective head fire was not observed as shown in Figs. 9a and 9b. This feature was attributed to the heterogeneity of the vegetative structure of the plot, which was not the case in their experiment. It is discussed in the subsection concerning the vegetation effects on the fire spread. In Figs. 9a and 9b, the "effective head fire width" and maximum rate of spread are defined, like in [11] as follow: the effective head fire width is the width of the fire, measured at right angles to the direction of head fire spread and the maximum rate of spread is determined by measuring the minimum distance between perimeters normal to the previous perimeter.

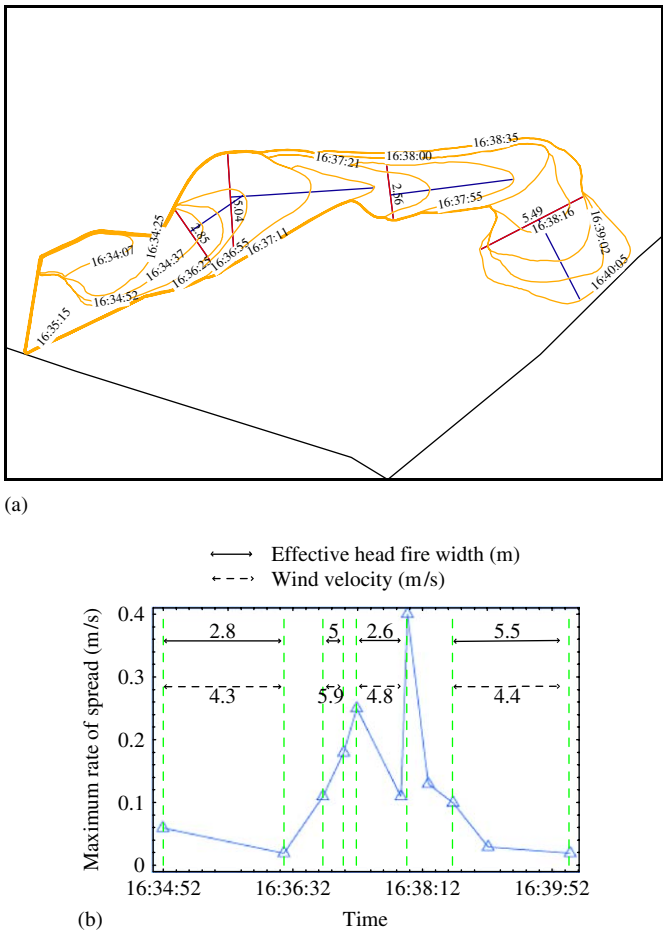

Fig. 9. Effective head fire width defined as the width of the fire front, which influences the next period of head fire spread (a) and maximum rate of spread measured normal to the previous isochrone (b).

4.2. Wind effects on the fire behaviour

It is well known that rate of fire spread increases with wind velocity [24,26]. The reason is to be found in the following fundamental mechanisms of combustion, heat transfer and kinetics of thermal degradation of fuel. Combustion is controlled by the oxygen and volatiles supplied to the reaction zone. The arrival of oxygen depends on the wind direction and intensity or/and on the natural convection created by the rising hot plume. The higher the wind speed, the higher the combustion efficiency and the bigger the heat released by the flame. The release of gaseous fuels depends on the heating and pyrolysis of the vegetation ahead of the flame and their convection and diffusion to the reaction zone. Heating of the fuel depends on the heat transfers from the flames to unburned fuel by radiation and convection. If wind is blowing in the same direction as the fire front advance, flames are tilted forward and are brought closer to the unburned fuel, increasing the radiation impinging on the fuel, the preheating range (leading to faster release of volatiles) and thus the rate of spread. Furthermore, the convective hot gases from the flame also heat the fuel.

Measurements provided by the three sonic anemometers revealed that there were just a few spatial variations of wind speed and direction between those sensors during the course of the fire. Hence, in order to discuss the wind effects on fire behaviour, we will consider the measurements of the anemometer located on the right side of the parcel. It was not submitted to the wind produced by the fire, which spread downward and provided information on the wind blowing directly through the flame zone and influencing the fire. Wind speed and direction from that sensor are displayed, respectively, in Figs. 10a and 10b over the duration of the experiment. We can see that there was a variation on local wind conditions both on speed and direction. Wind velocities were always in the low to moderate range and varied between 2 and 6 m/s at this location. Wind direction shifted from southwest to northwest and reciprocally over time.

In order to evaluate the wind influence on fire spread, we have superimposed in Figs. 10a and 10b, the four periods of time for which the fire stopped (identified from video analysis). Three of these time intervals correspond obviously to low wind speeds (lower than 3 m/s in average), but the first one occurred during moderate wind activity (mean wind speed of 4.5 m/s) for which fire spreads the rest of the time. The reason for this stopping in fire spread is to be found in the vegetation effects and will be detailed in the

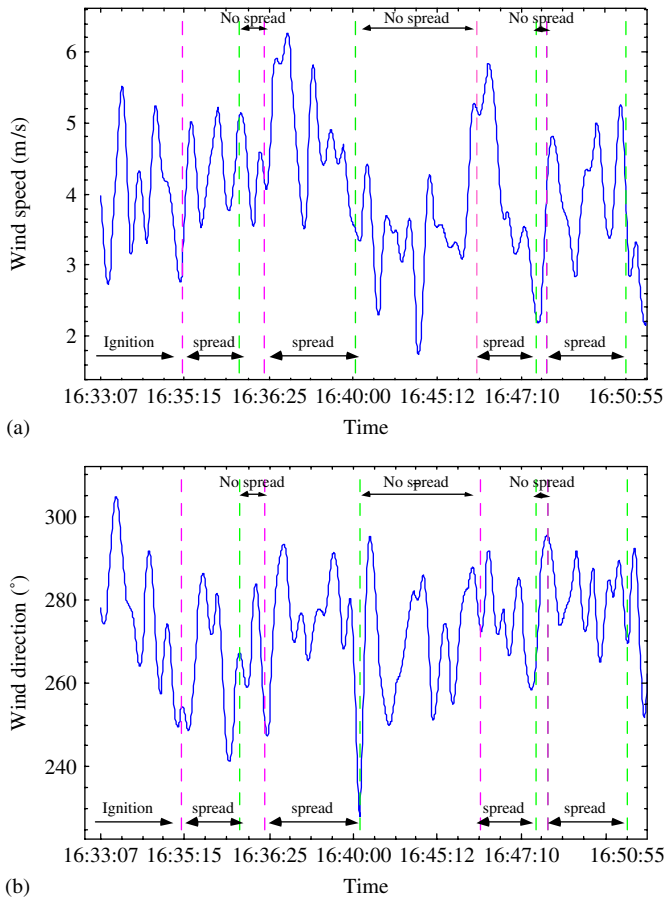

Fig. 10. Wind direction (a) and speed (b) on the right side of the plot over the duration of the experimental fire.

next section. With regard to the periods of time associated with fire propagation, we can note that highest rates of spread are strongly correlated with highest wind speeds (see Figs. 8 and 10a at time intervals [16:36:25,16:38:00] and [16:45:12,16:45:37]). At those moments, the surface wind was able to overcome the fire's buoyancy resulting in tilted flames (far from vertical), increasing the heat transferred towards the unburned fuel resulting in accelerating the fire rate of spread. This feature is clearly demonstrated by Fig. 11, which shows a flame tilted by the wind. Conversely, we could observe that while spreading periods for which the wind speed decreased to values lower than 3 m/s, the flames were not sheared away by the wind. This result corroborates the work of [27]. These last authors stated that the extent to which a fire can remain separate from the ambient wind field largely depends on the intensity of the fire to overcome the horizontal and mixing forces in the wind field through which the gases pass.

Figs. 8, 10a and 10b show that the main directions of wind and fire are strongly correlated. During the first period of spreading, the fire was driven by the west/southwestern wind. During the second period of fire activity the wind shifted from west/southwest to west/northwest, and the fire turned on the right. Vegetation effects further increased this change in fire spread. Finally,

Fig. 11. Flame tilted by the wind.

the wind shifted again in the third and fourth spreading period from west/northwest to west causing another change in the direction of the head fire, which turned on the left. This last change in wind direction is displayed by Figs. 10a and 10b where the peaks in wind velocities, up to 5 m/s (Fig. 10a), are clearly associated with western wind (angles of about 270° in Fig. 10b). At this point, it should be mentioned that the size of the plot was sufficient to allow a free propagation. The wedge-shaped front characteristic of restricted fires in their lateral development was not observed. This was the case even for the last part of the spreading for which the fire developed a broad parabolic head (see Fig. 8b at time 16:48:27) in spite of the lack of available fuel in the upper limit of the parcel. The plot size allowed accommodating the head fire shape that resulted from shifts in wind direction.

4.3. Vegetation effects on the fire behaviour

We noticed two important effects of vegetation on the fire spreading. They were most probably increased because of the high moisture content of vegetation due to the rainy conditions during the last spring. The first one concerns the rate of spread and the second one deals with the change in direction.

The first effect was observed during the first fire attenuation (time interval [16:35:25,16:36:10]) that corresponded to the entering of the fire in a zone constituted mainly by groves of *O. Europaea* (surrounded in red in Fig. 8a). As noticed in the previous section, we observed a break in fire spread during a time of moderate wind activity on the parcel for which fire spreads the rest of the time. We attribute this behaviour to the high moisture content of this species (see Table 1) and to the low preheating effect of small flames from the lower shrub layer on its foliage. Indeed, *O. Europaea* groves are 1–1.5 m higher than the species of the lower shrub layer (see Table 1). The flames

were particularly small because of the presence of a *Cistus Monspeliens* grove surrounding the *O. Europaea* one. Usually *C. Monspeliens* supports fast-spreading fires, but only when it is dry. During the experiment, we noticed that the fire was particularly slowed down by this species and we attributed this behaviour to its high moisture content (see Table 1) that led to low intensity fires. Reduced fire spread rates were also observed during the second spreading with two other *O. Europaea* groves (surrounded in red in Fig. 8b) that induced a curving of the fire front.

The second effect was observed during the time interval [16:37:21,16:38:00]. An acceleration of the fire trough a *C. Triflorus* grove (cf. Fig. 8a, grove surrounded in green) involved a slight change in direction of the fire. This growing in fire intensity allowed the adjacent *O. Europaea* grove (surrounded in dashed red) and the adjacent *Q. Ilex* trees to start burning. However, the main effect of vegetation on the fire direction was observed just after, between times [16:38:00,16:40:05]. The wind was blowing approximately in the 280° direction (cf. Fig. 10b) and the fire followed a direction of 315–320°. We attribute this behaviour to the presence of the *O. Europaea* grove (surrounded in dashed red lines in Fig. 8a) located on the left side of the fire front. This grove acted as an inhibition zone and did not allow the fire to propagate quickly in its direction. The resulting change in direction ranged between 35° and 40° from the wind direction.

Conversely, under other conditions, the fire passed through groves of the upper layer without slowing down (look at examples surrounded in purple in Figs. 8a and 8b). This effect can be explained by considering both the immediate groves vicinity and the wind velocity. Indeed, when shrubs that burned easily surrounded a plant or a grove, the plant or grove received a great amount of energy, and then dried and burned quickly. This result was observed at the beginning of the first spreading (corresponding to the time interval [16:33:07,16:34:25] in Fig. 8a), when the fire advanced slowly but single plants of *Q. Ilex* bordering *E. Arborea* and *A. Unedo* groves burned. *E. Arborea* and *A. Unedo* burned easily and induced flames high enough to ignite the upper layer. Between time intervals [16:36:25,16:38:00] and [16:45:12,16:45:37], the fire also passed quickly through *Q. Suber*, *Q. Ilex* and *O. Europaea* groves (surrounded in purple in Figs. 8a and 8b) and went straight away, following the wind direction. These two intervals correspond to the higher wind speeds observed during the experiment (cf. Fig. 10a).

Another effect should be mentioned for the species of the upper layer. They presented a long induction phase before ignition (and sometimes no ignition at all) and sometimes we observed a torching effect of groves (as the groves of *Q. Suber* surrounded in blue in Fig. 8b). It induced spotting, as mentioned in the previous section. Concerning the grass layer, it had no influence when fire spread but played a great role in some attenuation intervals as it sustained the fire. Indeed, it was the single burning layer and thanks to wind squalls, the fire started again from it. Finally, because of the heterogeneity of vegetation, we did not observe several effects mentioned in other works for quite homogeneous shrublands. For instance, the increase in rate of spread with a wider effective head fire was not observed as mentioned here before in the section "time history of the fire front". The effect that the wetter fuel type acted to curb the intensity of the fire as noticed by [28] was not observed too. Indeed, even if the moisture content had an influence on the fire spread for a single species (as mentioned here above for *Cistus Monspeliens*), the heterogeneity of vegetation played an important part on the fire dynamics. For instance, the species of the lower shrub layer that burned the best was *Cytisus Triflorus* even if it was in the wettest state (see Table 1).

These results allow us to state that the heterogeneity of the vegetation played a great role in fire spread and involved different behaviour such as: speeding up or down the fire, changing its direction and inducing layer effects.

4.4. Fire intensity and fire impact

In this section we just provide estimates of characteristic quantities, as we did not measure some physical parameters directly. Fire intensity kW/m) was calculated by using Byram's equation [19]:

$$I = HWR, \tag{1}$$

where H is the heat of combustion associated with the species (kJ/kg), W is the weight of the fuel consumed per unit area (kg/m^2) and R is the rate of spread (m/s). A basic value of 19500 kJ/kg was used for low heat of combustion with a reduction for moisture content [29]. W was estimated from data concerning similar species [30,31]. We set it to the weight of the fine particles of vegetation as we noticed that they were totally consumed by the fire, whereas the thicker ones did not burn. R was calculated as the ratio between distance and time for two successive positions of the fire front (cf. Fig. 9b). To reinforce our estimations, we used also the following approximate relation between flame length, L (m) and fire-line intensity [29]:

$$I = 259.8L^{2.174}, \tag{2}$$

where L (m) is the mean flame length estimated from video analysis.

Two periods of time corresponded to high fire-line intensities (as instantaneous values). The first one occurred while the fire spread through a *Cytisus Triflorus* gorse (surrounded in green in Fig. 8a at time 16:37:55) with a strong velocity and the second one to the burning of a gorse of *O. Europaea* (time 16:38:16). The two values of I, estimated from an average between results from Eqs. (1) and (2), are, respectively, $I = 20500$ kW/m (with $R = 0.4$ m/s, $W = 3$ kg/m^2 and $L = 7.5$ m) and $I = 19000$ kW/m (with $R = 0.1$ m/s, $W = 10$ kg/m^2 and $L = 7.4$ m). These two values are higher than the ones recommended for prescribed burning [29] and can be

encountered in wildland fires. Conversely, we observed (cf. Figs. 10a and 10b) intensities lower than 1000 kW/m in attenuation periods. This value is indicative of the low-intensity surface fire category suggested for most prescribed fires.

Concerning fire severity we could not evaluate it directly because we just measured the temperature near the ground (5 cm above it). However, we observed flame residence times around 1 min and temperatures near the ground higher than 150 °C during 5 min because of the presence of embers and hot ashes on the ground. Knowing that the soil was quite dry and that all the fine particles of vegetation were burned (leaves, twigs of shrubs and the entire grass layer) in the area of fire spread, we can assume a quite high fire severity compared to other shrubland fires [32].

Fire impact can be analysed, thanks to radiant heat fluxes recorded, at 5, 10 and 15 m from the upper limit of the plot. We consider here the heat flux sensors located 2 m above the ground because it corresponds to the height of a standing person. Fig. 12 allows us to argue that the safety distance for exposed people should be more than 5 meters from the fire front. Indeed, the sensor located at 5 m from the plot measured a peak value of the radiant heat flux of 7.5 kW/m^2. This value is greater than 6.4 kW/m^2 for more than 8 s, which is the limit of time to feel pain on skin exposed to 6.4 kW/m^2 [33]. At 10 m from the plot, the maximum heat flux measured was 3 kW/m^2. This value corresponds to pain felt on exposed skin after 120 s [33]. This heat flux was not observed for that period of time during that part of the fire spread. At 15 m, the peak of the heat flux is twice the summer sunshine in the Mediterranean. The residence times measured in the experiment proved that firefighters could have stayed on the fuel break at a distance of 5 m from the fire front. Indeed, the maximum exposure for a firefighter wearing firefighting clothing during 90 s is 7 kW/m^2 [34] and the heat flux was over this value for just a few seconds.

As the experiment was conducted after an exceptional rainy spring, the values of the measured radiant heat fluxes remain to be verified in the future with fires under dryer vegetation conditions.

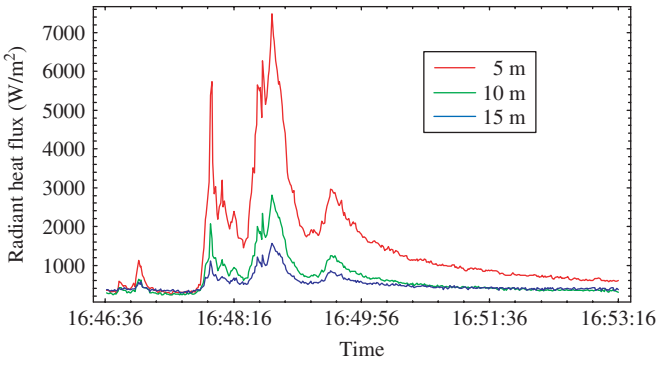

Fig. 12. Radiant heat flux recorded at two meters high ahead of the fire front for the second head shape.

4.5. Structure of the fire plume

The "thermocouple trees", built to study the temperature with height during the fire plume formation process, obviously require the fire to enter the measuring section and that the flames remain vertical long enough to observe the relevant phenomena. However, one of the disadvantages inherent to field experiment is the impossibility of having control over the meteorological conditions. Either a small shift in wind direction or a strong wind speed overcoming the fire plume could make the fire avoid the measuring structures or stretch the flame and alter the measurements. For instance, the first "thermocouple tree" placed on the right side was not reached by the fire. Concerning the second and third ones located, respectively, in the middle and on the left side of the plot, there were variations on local wind conditions when the fire reached them, one after the other. Lulls in wind occurred at those times. The wind speed decreased to less than 3 m/s and the fire plume overcame the surface wind. The profiles recorded present similar temperature with height and only the measurements provided at the third mast will be discussed since the flames remained vertical for a long time at that location (up to 20 s).

A qualitative description of the burning processes, with reference to Fig. 13a, which presents the temperature curves of thermocouples number 1 and 3 located in the vegetation (at 0.6 and 1.8 m height), is first provided to describe the spreading features. The thermocouple curves reveal a temperature increase as the fire approaches until it reaches them. Heat is transferred from the flames to the unburned fuel, the temperature of which increases. When this fuel becomes hot enough, it pyrolyzes. The resulting gaseous fuel reacts once it comes into contact with oxygen when it is hot enough and a flame ensues. The signals fluctuate around average maximum values, meaning that the sensors are immersed in the flame. After this zone, which lasts several seconds (depending on fuel conditions), the flame decreases in size and hence temperature, due to a lack of readily available fuel. We can notice the fire first reaches thermocouple 3, which is located above thermocouple 1 (see Fig. 13a). This result demonstrates that the top of the vegetation is licked by flame before the whole shrub layer is included in the flaming zone. It points out that the fire plume leans towards the unburned fuel, because the upper thermocouple responds before the lower one. Then, when the whole shrub ignites the two thermocouples are immersed in the flame.

Fig. 13b shows the distribution of the vertical temperature over time, during part of this stage (time interval [16:48:30,16:48:42]), for eight of the ten available levels (0.6; 1.2; 1.8; 2.4; 3.0; 3.6; 4.8; and 6 m), simplifying the analysis. The first three levels (thermocouples number 1–3) take place inside the vegetation zone while the others (thermocouples 4, 5, 6, 8 and 10) are located above it. Those results show the three classical behavioural regions encountered in free burning fires. The lower part of the fire

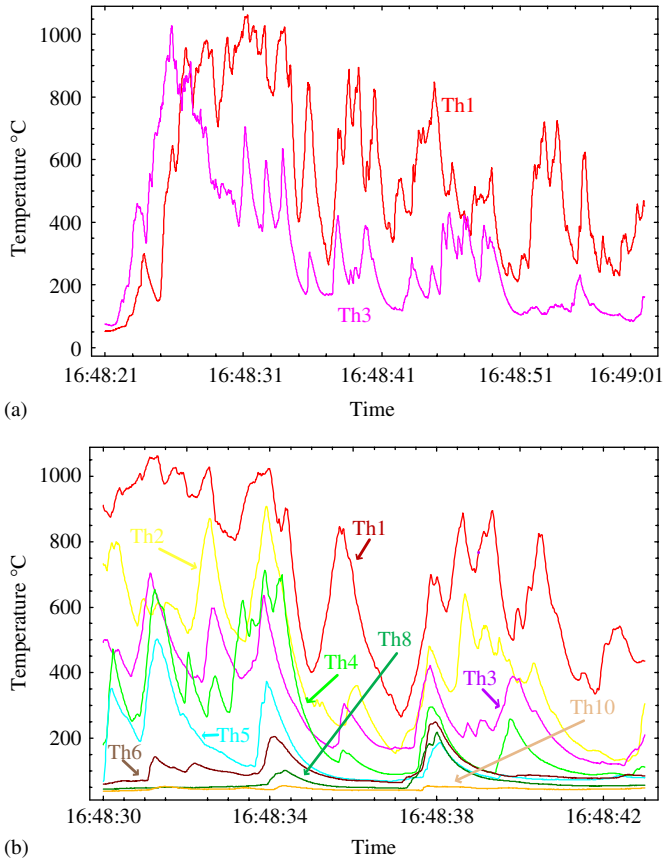

Fig. 13. Gas temperature: over time at 0.6 and 1.8 m height in the vegetation when the fire plume comes through the third "thermocouple tree" (a) and over time along the fire plume axis at the third "thermocouple tree".

plume is the continuous flame region containing the vegetation zone where the temperature is maximum reaching 1060 °C for thermocouple 1, 2 and 3 (see Fig. 13a for probe 3). Over that region, there is the intermittent one, where balls of flame come away from the source. This zone includes thermocouple 4 and 5 where the temperature grows up to 700 °C. During this short time interval it is not visible for thermocouple 5 but other time intervals make it clearer. The upper part (from the height of 3.6 m) is the beginning of the conventional thermal plume. Thermocouples 6–10 belong to this region, the cooling of which is mainly due to entrainment and mixing of ambient air.

It should be pointed out that important discrepancies appear between those results and data from laboratory scale experiments [8]. In the latter, we could see that the temperature greatly fluctuates above the fuel. These fluctuations were attributed to the turbulent feature of the flow above the ejection zone of the pyrolyzate gases. This pattern was not encountered here. The reason may to be found in the scale of the eddy structures originating from the flames at field level that are bigger than those observed for small-scale laboratory fires. The puffing frequency of the fire plume (calculated from the fluctuations of the temperature curves) was about 1–2 Hz at the field scale while it could reach 5 Hz at the laboratory scale. Furthermore, the temperature increase just above the vegetation mentioned by different authors [8,35] for small pine needle fuel beds was not observed. This last characteristic was attributed to an oxygen deficit due to the ejection of the pyrolyzate gases, which makes the combustion incomplete. It was not the case in our experiment where the mixing with fuel and oxidant seemed sufficient, even in the vegetative structure, to provide the highest temperature in this region.

5. Conclusion

The main contributions of this work can be summarized as follow: simple and sound experimental devices were built to investigate the fire front shape, its rate of spread, the amount of energy impinging ahead of it, the vertical distribution of the temperature within the fire plume, as well as the wind velocity and direction during the spreading of a fire. Wind and vegetation effects on fire behaviour were described. Fire plume pattern was also investigated. All data presented here can be viewed as part of a necessary set dedicated to understand the fire behaviour and its main properties and relation to the weather conditions, the vegetative structure and the topography. Only few of the measured thermodynamics quantities were reported and analysed in this article. The other will be presented in a subsequent paper, the scope of which is devoted to learn how to capture the driving physical processes, most of which are very small in scale compared to extensive fires. Although small-scale experimental fires on plots of fixed size and configuration do not duplicate actual wildfire, the set of results provided in this paper can be considered as an important contribution to test, to validate and to tune models of wildland fire. Whether one considers statistical, empirical or physical models, the present data can be used to compare the ability of these models to predict the fire behaviour descriptors such as the flame properties, the flame residence time, the Byram's fireline intensity and the fire front shape as well as the thermodynamic quantities involved in fire. This work represents our research team's first step in conducting field experiments devoted to provide reliable thermodynamic data on fires. Although this paper deals essentially with one experimental fire, the results are valuable and met our twofold objectives: we tested our original and innovative measuring devices built in for field experiments investigation and we brought a new contribution to the forest fire scientific community upon the knowledge of thermodynamics quantities involved in a field fire. Further studies will be conducted in the future, both to improve the proposed protocol and to obtain more data on similar and other vegetative structures, as detailed fuel loading, size and distribution along the height that are necessary to tune multiphase models.

Acknowledgements

The authors would like to acknowledge the support provided by the local government of Corsica (CTC)—Grant No. 1-3732. This field experiment also required the cooperation of a large number of people and would not have been possible without the assistance of:

1. The Forestry Service Department of South-Corsica, which constructed firebreaks and protected the area and especially Jean-Yves Duret, who conducted the burning.
2. The Firemen of Santa Lucia di Porti Vecchju, who protected the area and carried out fire suppression when spotting occurred.
3. The Forestry (ONF) and Agriculture (DDAF) Services, which sustained this project since the beginning.

We also would like to acknowledge Doctors J.P. Vantelon and J.P. Garo, from the LCD of Poitiers (UPR CNRS 9028), who made valuable recommendations on field scale measurements.

References

[1] Weber RO. Modelling fire spread through fuel beds. Prog Energy Combust Sci 1990;17:67–82.
[2] Grishin AM. Mathematical modelling of forest fires. Num Meth Cont Mech 1978;9:30–56.
[3] Grishin AM. Mathematical modeling of forest fires and new methods of fighting them. Tomsk State University: Publishing House of the Tomsk State University; 1997.
[4] Larini M, Giroux F, Porterie B, Loraud JC. A multiphase formulation for fire propagation in heterogeneous combustible media. Int J Heat Mass Trans 1998;41:881–97.
[5] Bellemare LO, Porterie B, Loraud JC. On the prediction of firebreak efficiency. Combust Sci Technol 2001;163:131–76.
[6] Sero-Guillaume O, Margerit J. Modelling Forest fire: Part 1 and Part 2. Int J Heat Mass Trans 2002;45:1705–37.
[7] Porterie B, Morvan D, Loraud JC, Larini M. Firespread through fuel beds: Modeling of wind-aided fires and induced hydrodynamics. Phys Fluids 2000;12:1762–81.
[8] Marcelli T, Santoni PA, Simeoni A, Leoni E, Porterie B. Fire spread across pine needle fuel beds: characterization of temperature and velocity distributions within the fire plume. Int J Wildland Fire 2004;13:37–48.
[9] Morvan D, Dupuy JL. Modeling the propagation of a wildfire through a Mediterranean shrub using a multiphase formulation. Combust Flame 2004;138:199–210.
[10] Cheney NP, Gould JS, Catchpole WR. The influence of fuel, weather and fire shape variables on fire spread in grasslands. Int J Wildland Fire 1993;3(1):31–44.
[11] Cheney NP, Gould JS. Fire growth in grassland fuels. Int J Wildland Fire 1995;5(4):237–47.
[12] Clark TL, Jenkins MA, Coen J, Packham D. A coupled atmosphere-fire model: convective feedback on fire line dynamics. J App Met 1996;35:875–901.
[13] Linn RR, Reisner J, Colman J, Winterkamp J. Studying wildfire behavior using firetec. Int J Wildland Fire 2002;11(4):233–46.
[14] Marsden-Smedley JB, Catchpole WR. Fire behaviour modelling in Tasmania buttongrass moorlands. I & II. Fuel characteristics. Int J Wildland Fire 1995;5(4):203–28.
[15] Carrega P. Relationships between wind speed and the R.O.S. of a fire front in field conditions: an experimental example from the Landes forest, France. Forest fire research—Proceedings of the fourth international conference, 2002. CD ROM.
[16] Loureiro C, Fernandes P, Botelho H. Optimizing prescribed burning to reduce wildfire propagation at the landscape scale. Forest Fire research—Proceedings of the fourth international conference, 2002. CD ROM.
[17] Viegas DX, Cruz MG, Ribeiro LM, Silva AJ, Ollero A, Arrue B, et al. Gestosa fire spread experiments. Forest fire research—Proceedings of the fourth international conference, 2002. CD ROM.
[18] Alexander ME, Stocks BJ, Wotton BM, Flannigan MD, Todd JB, Butler BW, et al. The international crown fire modelling experiment: an overview and progress report. Fire and forest meteorology—Proceedings of the second symposium, American Meteorological Society; 1998. p. 20–3.
[19] Byram GM. Combustion of forest fuels. In: Davis KP, editor. Forest fire control and use. New York: McGraw-Hill Book Company; 1959. p. 61–89.
[20] Miranda AI, Borrego C. Air quality measurements during prescribed fires. Forest fire research—Proceedings of the fourth International conference, 2002. CD ROM.
[21] Van Wagner CE. Conditions for the start and spread of crown fire. Can J Forest Res 1977;7(1):23–34.
[22] Bovio G, Camia A. An analysis of large forest fires danger conditions in Europe. Forest fire research—Proceedings of the third international conference, 1998. p. 975–94.
[23] Dupuy JL, Maréchal J, Morvan D. Fires from a cylindrical forest fuel burner: combustion dynamics and flame properties. Combust flame 2003;135:65–76.
[24] Mendes-Lopes JMC, Ventura JMP, Amaral JMP. Flame characteristics, temperature-time curves and rate of spread in fires propagating in a bed of Pinus pinaster needles. Int J Wildland Fire 2003;12:67–84.
[25] Carvalho A, Miranda AI, Borrego C, Santos P, Amorim JH, Viegas DX. Fire as a heat source to the atmosphere: measuring and modelling. Forest fire research—Proceedings of the fourth international conference, 2002. CD ROM.
[26] Viegas DX. On the existence of a steady state regime for slope and wind driven fires. Int J Wildland Fire 2004;13:101–17.
[27] Chandler C, Cheney P, Thomas L, Williams D. Fire in forestry: forest fire behaviour and effects. 2nd ed. Malabar: Krieger Publishing Company; 1991.
[28] Baeza MJ, de Luis M, Raventós J, Escarré A. Factors influencing fire behaviour in shrublands of different stand ages and the implications for using prescribed burning to reduce wildfire risk. J of Env Management 2002;65:199–208.
[29] Alexander ME. Calculating and interpreting forest fire intensities. Can J of Botany 1982;60:349–57.
[30] Brown JK. Bulk densities of nonuniform surface fuels and their application to fire modelling. Forest Sci 1981;27(4):667–83.
[31] Papió C, Trabaud L. Comparative study of the aerial structure of five shrubs of Mediterranean shrublands. Forest Sci 1990;37(1):146–59.
[32] Pérez B, Moreno JM. Methods for quantifying fire severity in shrubland-fires. Plant Ecol 1998;139:91–101.
[33] Drysdale D. An introduction to fire dynamics. Chichester: Wiley; 1985. p. 57.
[34] Cohen JD, Butler BW. Modeling potential structure ignitions from flame radiation exposure with implications for wildland/urban interface. Fire management—Proceedings of the thirteen fire and forest meteorology conference, Lorne, Australia, 1996, p. 81–6.
[35] Dupuy JL, Maréchal J, Bouvier L, Loïs N. Measurement of temperatures and radiant fluxes during static fires in a porous fuel. Forest fire research—Proceedings of the third international conference, 1998. p. 843–58.